



HAL
open science

DROPIC: A tool for the study of string instruments in playing conditions

Jean-Loic Le Carrou, Delphine Chadefaux, Marie-Aude Vitrani, Sylvère Billout, Laurent Quartier

► **To cite this version:**

Jean-Loic Le Carrou, Delphine Chadefaux, Marie-Aude Vitrani, Sylvère Billout, Laurent Quartier.
DROPIC: A tool for the study of string instruments in playing conditions. Acoustics 2012, Apr 2012, Nantes, France. hal-00811154

HAL Id: hal-00811154

<https://hal.science/hal-00811154>

Submitted on 23 Apr 2012

HAL is a multi-disciplinary open access archive for the deposit and dissemination of scientific research documents, whether they are published or not. The documents may come from teaching and research institutions in France or abroad, or from public or private research centers.

L'archive ouverte pluridisciplinaire **HAL**, est destinée au dépôt et à la diffusion de documents scientifiques de niveau recherche, publiés ou non, émanant des établissements d'enseignement et de recherche français ou étrangers, des laboratoires publics ou privés.



ACOUSTICS 2012

DROPIC: A tool for the study of string instruments in playing conditions

J.-L. Le Carrou^a, D. Chadeaux^a, M.-A. Vitrani^b, S. Billout^a and L. Quartier^a

^aEquipe LAM - d'Alembert, 11, rue de Lourmel, 75015 Paris, France

^bInstitut des Systèmes Intelligents et Robotique, Université Pierre et Marie Curie - Paris VI
Boite courrier 173 4 Place Jussieu 75252 Paris cedex 05
jean-loic.le_carrou@upmc.fr

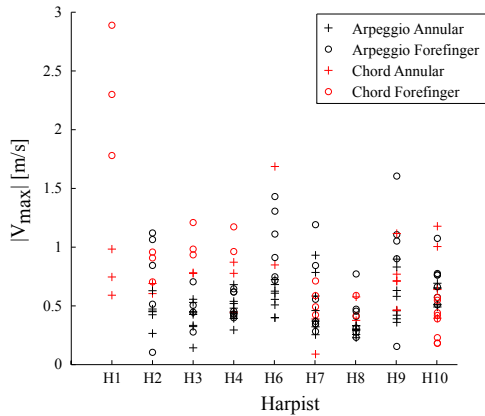


Figure 2: Maximum velocity computed for each repetition of chord or arpeggio sequences for each of the 10 harpists.

a fundamental frequency at 138.6 Hz), we estimate that the force magnitude can be up to 15 N.

3 Description of DROPIC

In this section, we describe the robotic finger that we develop to reproduce the harpist's plucking action. From the results presented in Section 2, we can draw the DROPIC's specifications that will have an impact on the mechanical and control design.

3.1 Specifications

We summarize here the main specifications of DROPIC that we defined thanks to the measurements performed on the ten harpists:

- Area of use: $20 \times 20 \text{ mm}^2$
- Maximum velocity of the fingertip: 1.5 m/s
- Maximum force of tension: <15N

Note that, for a robot, the combination of high speed displacement, and accuracy with a 15 N load is not yet straightforward.

3.2 Mechanical description

To reproduce the finger's trajectories, a planar robot with two rotational joints (RR-robot) is chosen. This kind of robot, schematized in Figure 3-(A), is composed of 2 arms connected by two pivots. The knowledge of the angular position of each pivot allows a perfectly controllable 2-dimensional movement. The extremity of the 2nd arm, labeled P in Figure 3-(A), has to describe the same trajectory as that of the harpist's finger. The angular positions of each arm, denoted θ_1 and θ_2 in Figure 3-(A), are evaluated with a straightforward geometrical model (compatible with our configuration):

$$\theta_1 = \arctan\left(\frac{z_f(l_1 + l_2 \cos(\theta_2)) - x_f l_2 \sin(\theta_2)}{x_f(l_1 + l_2 \cos(\theta_2)) + z_f l_2 \sin(\theta_2)}\right) \quad (1)$$

$$\theta_2 = -\arccos\left(\frac{x_f^2 + z_f^2 - (l_1^2 + l_2^2)}{2l_1 l_2}\right) \quad (2)$$

where l_1 and l_2 are the arms' lengths, and (x_f, z_f) the fingertip coordinates.

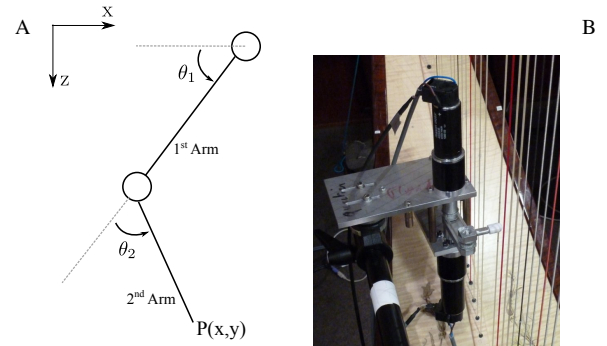


Figure 3: Kinematic description of DROPIC (A) and picture of DROPIC set up on the concert harp (B).

Angles θ_1 and θ_2 are driven by two motors placed at the robot's base for compactness reasons (see a picture of DROPIC in Figure 3-(B)). The transmission of the motor's torque to the second joint is carried out by a belt. The arm's length is chosen to be of the same order of magnitude as the last two phalanxes of a human forefinger. Eventually, we chose $l_1 = l_2 = 45 \text{ mm}$ which fulfill the first specification, i.e. the end effector (denoted P in Figure 3-(A)) can perform all trajectories in a 400 mm^2 area. The motors and the reducers are chosen according to the expected motor's torque. The latter is derived from the second arm length and the maximum load at the end effector, which is overestimated by a security margin of 10 N. Besides, to ensure the position-control of the robot, angular encoders are added to reducers. Finally, DROPIC is fixed rigidly to the harp by an arm connected to the pillar, as shown in Figure 3-(B).

3.3 Control description

The implemented control law is represented in Figure 4. At the lowest level, a Proportional-Integral controller allows to control the current, which is proportional to the torque delivered by the motors. The matrix $\begin{pmatrix} \frac{1}{N_1 K_{C1}} & 0 \\ 0 & \frac{1}{N_2 K_{C2}} \end{pmatrix}$ is used to specify a desired torque and to compute the corresponding current to be sent in the motors.

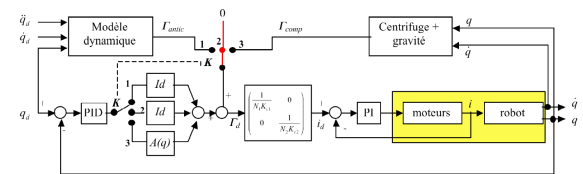


Figure 4: implemented control law

At the highest level, this scheme allows to carry out three different controllers, ensuring the calculation of the desired torque as a function of the wanted position and the current position:

- When K is set to 2, the position-control is a simple decentralized Proportional-Integral-Derivative controller.
- When K is set to 1, the command is identical to the earlier, with the addition of a term of dynamics anticipation. As the friction is not repeatable, it is not included in the dynamic model.

- When K is set to 3, the control is performed by dynamical decoupling.

The two first control laws are used to manually tune the gains of the controller. The third control law is used to execute a desired trajectory, as shown in Figure 5.

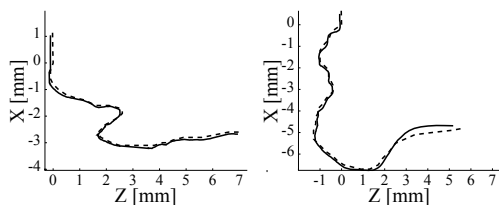


Figure 5: Two Examples of DROPIC's end-effector trajectory measured by the rotary encoders (solid line) compared to the reference (dashed line).

3.4 Fingertip description

The robotic fingertip shape and material are of a great importance since it defines the friction behavior between the finger and the string. Thus, it is designed as an aluminum bone on which a piece of silicone can be slipped on. Silicone is chosen because of its moulding's facilities and the large amount of mechanical properties which is accessible thanks to its composition. Moreover, it has been shown that silicone and human skin have common properties [6]. In the following, we use a parallelepiped-shaped or a cylindrical-shaped fingertip.

4 Validation

In this section, we set out to validate DROPIC as a tool to study the harp in playing condition. First, we study the repeatability and the accuracy of DROPIC in comparison to the harpist. Secondly, we are interested in the sound produced by the plucks performed by DROPIC.

4.1 Experimental setup

In order to measure the DROPIC's fingertip trajectory and the produced sound, an experimental protocol based on that previously used in [5] is set up. A high-speed camera is used for filming DROPIC, as shown in Figure 6, set at 5167 frames per second. Simultaneously, an accelerometer, located at the bottom of the plucked string, measures the soundboard vibrations. A particular image processing is implemented to track markers on the fingertip and on the string to obtain the trajectories, as described in [5].

4.2 DROPIC's repeatability

As shown in Figure 7-(A), each harpist provides a reproducible finger's movement when s/he plucks a string [5]. Hence, DROPIC must be at least as repeatable as a real musician. A repeatability average error, denoted $\bar{\epsilon}_d$, is computed after standard ISO 9283 [7, 8] to quantify DROPIC's performance:

$$\bar{\epsilon}_d = \frac{1}{N} \sum_{t=1}^N \sqrt{(X_r(t) - X_p(t))^2 + (Z_r(t) - Z_p(t))^2}, \quad (3)$$



Figure 6: Experimental setup

where (X_r, Z_r) and (X_p, Z_p) are reference and DROPIC trajectories (obtained by the encoders and equations 1 and 2), respectively. For the trajectory represented in Figure 7-(B), $\bar{\epsilon}_d$ is estimated to $0.18 \cdot 10^{-3} \pm 0.015 \cdot 10^{-3} \text{m}$ when a string is plucked. The reported repeatability uncertainty represents a 95% confidence interval. In order to compare the repeatability of DROPIC and of a musician, the dynamic time warping algorithm [9] is computed. This algorithm compares similarity between two signals which may vary in velocity and duration. DROPIC is found to be about 82 times more repeatable than the harpist, which fulfill the repeatability objective.

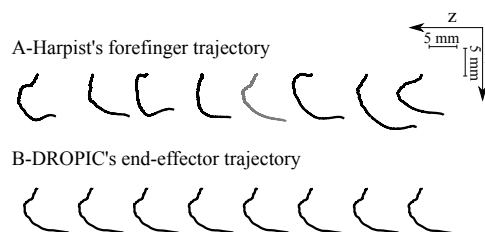


Figure 7: Repeatability of harpist's finger (A) and DROPIC end-effector trajectories (B). The plucks performed by DROPIC use the grayed harpist trajectory as reference

4.3 DROPIC's reliability

The reliability of the robotic finger to reproduce a real finger's trajectory is an important point to validate. In Figure 8, an example of DROPIC's trajectory measured by encoders and by a high-speed camera is compared to a reference one. We show that without string, the trajectory is perfectly carried out. However, when a force is applied to DROPIC's fingertip due to the string, a deviation of the robotic finger occurs. This force increases while the finger pulls the string, i.e. during the sticking phase $[t_c, t_s]$. At time t_s , the string begins to slip on the fingertip and the force reaches its maximum. At this instant, the deviation is maximum as shown in Figure 8 for the encoders data. We can estimate this value at less than 1 mm for 9 N. Note that in Figure 8, DROPIC's trajectory measured by the high-speed camera shows an important deviation in comparison to that of the encoders. This is certainly due to the silicone fingertip deformation combined with the uncertainties related to the encoders and finger trajectories' measurement.

The global uncertainty of the displacement's measurements are quantified using the propagation of uncertainties

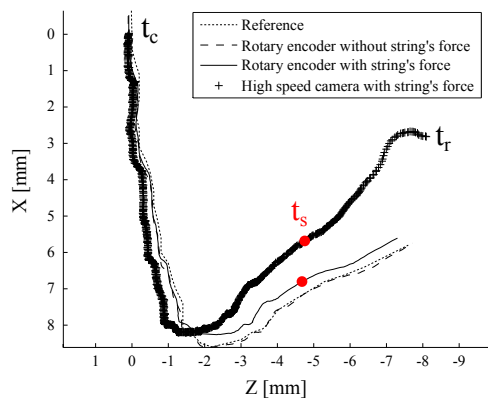


Figure 8: Example of a DROPIC's trajectory measured by the rotary encoders and by the high speed camera for two configurations: with and without a string.

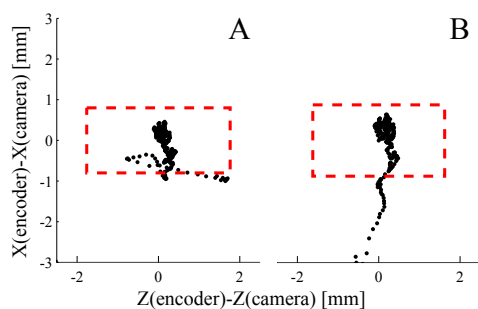


Figure 9: Distance between the DROPIC end-effector trajectories measured by the encoders and by the high-speed camera without string force (A) and with string force (B). The dashed red lines show the measurement uncertainties with a 95% confidence interval.

formula. For this purpose, the uncertainties of the markers' tracking, of the ratio between image's pixels and a distance known, of the angle between the camera's axis and the string's plane, of the resolution of encoders and of the length of each arm are estimated. In Figure 9, we show the uncertainty, with a 95% confidence interval, of the distance between the trajectory measured by the encoders and by the high-speed camera. Without a string, most of the point are inside the confidence interval. With a string, few points are outside the confidence interval due to the silicone's deformation during the slipping phase. This result shows that the encoder is a good estimator of the fingertip location except when the fingertip is deformed by the string's force. However, DROPIC's control has to be improved to increase its accuracy when the string's force is applied to the fingertip.

4.4 DROPIC's sound producing

In Figure 10-(A), we present the waveforms of an isolated note plucked by a harpist. The extracted finger's trajectory is then used as input reference for DROPIC. Three repetitions of this pluck are performed by DROPIC, see Figure 10-(B,C,D). These three repetitions are very similar, showing that DROPIC is perfectly repeatable. In comparison to the waveform obtained with the harpist, DROPIC have some differences as, for instance, the waveform magnitude. This can be explained by the fact that the pulling force on the string is highest for the harpist than for DROPIC. Therefore, the slipping phase begins earlier for DROPIC than for the

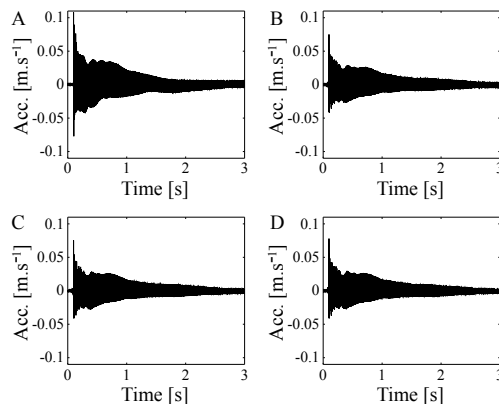


Figure 10: Accelerometer's signal measured at the connected point of the plucked string (Db 2) on the soundboard for a harpist (A) and for 3 repetitions of DROPIC (B), (C) and (D).

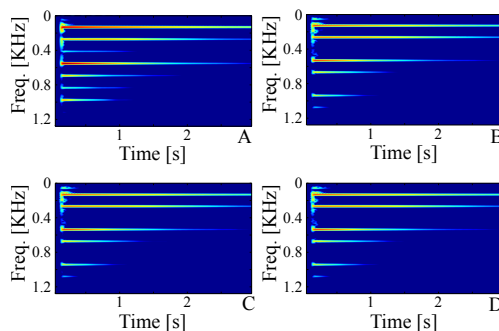


Figure 11: Spectrograms of Accelerometer's signal shown in Figure 10. Images are drawn in dB using a 70 dB dynamic.

harpist. This problem can be related to the trajectory and to DROPIC's fingertip material which does not have the same friction coefficient than the skin.

From a spectral point of view, we compute spectrograms of the four accelerometer's signals previously described, as shown in Figure 11. Note that on DROPIC's sound spectrograms the 3rd and the 6st harmonics are missing contrary to the harpist's sound. These differences are due to the slight variation in the DROPIC plucking position compared to the one of the harpist. Moreover, we see that the transient part of the signal is different between (A) and (B,C,D). Once again, this result emphasizes the differences occurring during the slipping phase between DROPIC and the harpist. Beyond the problem of DROPIC's trajectory, these results indicate that the fingertip's silicone can be improved in term of mechanical properties and of shape.

5 Conclusion

In this paper, we presented a new tool for plucking a harp string in playing conditions. This tool, called DROPIC, is a two rotational joints position-control robot which is able to carry out any trajectory of harpist finger. Its fingertip is made of silicone and can be changed as needed. Results indicate that DROPIC is perfectly repeatable but still requires improvement in the control to accurately follow an imposed trajectory when a string's force is present. Although sounds produced by DROPIC's pluck are convincing, the mechan-

ical properties and the shape of the silicone fingertip used have to be improved.

Acknowledgments

The authors acknowledge the harpists who participate in our studies on the harp: Marie Denizot, Pierrine Didier, Marie Klein, Sandie Leconte, Camille Levecque, Caroline Lieby-Muller, Magali Monod-Cotte, Blandine Pigaglio, Maëlle Rochut and Coralie Vincent. Thanks a lot for the help of Wael Bachta during the DROPIC's design and Maxime Harazi during the measurements.

References

- [1] D. Ferrand, C. Vergez, "Blowing machine for wind musical instrument: toward a real-time control of the blowing pressure", *IEEE Conference on Control and Automation*, 1562-1567 (2008)
- [2] D. Ferrand, C. Vergez, B. Fabre, F. Blanc, "High-precision regulation of a pressure controlled artificial mouth: the case of recorder-like musical instruments", *Acta Acustica united with Acustica* **96**, 700-711 (2010)
- [3] T. Smit, F. Türecikheim, R. Mores, "A highly accurate plucking mechanism for acoustical measurements of stringed instruments", *J. Acoust. Soc. Am.* **127**(5), EL222-EL226 (2010)
- [4] J. Woodhouse, "Plucked guitar transients: comparison of measurements and synthesis", *Acta Acustica united with Acustica* **90**, 945-965 (2004)
- [5] D. Chadeaux, J.-L. Le Carrou, B. Fabre, D. Daudet, "Experimentally-based description of harp plucking", *J. Acoust. Soc. Am.* **131**(1), 844-855 (2012)
- [6] S. Derler, U. Schrade, L.-C. Gerhardt, "Tribology of human skin and mechanical skin equivalents in contact with textiles", *Wear* **263**, 1112-1116 (2007)
- [7] NF EN ISO 9283: Robots manipulateurs industriels. Critères de performance et méthodes d'essai correspondantes (1998)
- [8] N.G. Dagalakis, "Industrial robotics standards", chapter 27, *National Institute of Standards and Technology*, 2003.
- [9] H. Sakoe, S. Chiba, "Dynamic programming algorithm optimization for spoken word recognition", *IEEE Transactions on Acoustics, Speech and Signal Processing* **26**, 43-49 (1978)